

5.3 Isophotal Twists in Elliptical Galaxies

The ellipticity of isophotes may vary with radius in the inner regions. Also, there may be a variation of major axis position angle (PA) of these isophotes with radius. The PA gives the orientation of the galaxy in the sky; it is the angle measured counterclockwise from north to the major axis, as shown in Figure 5.4.

A variation of PA with radius, or a twist, may be an indication of triaxiality, with no axis of rotational symmetry; see Figure 5.5. The bulge in M31 shows a twist in the major axis by about 10° near its center and has been fit by a triaxial model. M81 shows a similar small central twist, and near-infrared observations indicate that this may be common in spirals. Such twists may also be in-



FIGURE 5.4 Position angle is measured from the north counterclockwise to the major axis of a galaxy.

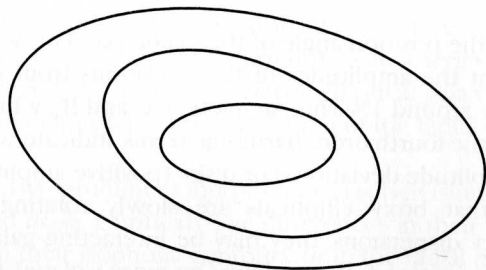


FIGURE 5.5 Some galaxies show isophotal twists and ellipticity variations with radius.

terpreted as an indication of the presence of small bars or nonaxisymmetric bulges in the central regions. This subject will be considered more fully in Section 5.10.

5.4 Radial Profiles for Spiral Galaxies

Spiral galaxies have bulges that are very similar to elliptical galaxies. The bulge surface brightness generally has the form $\log(\Sigma/\Sigma_0) \propto r^{-1/4}$, the same as for elliptical galaxies, although recent studies suggest that an exponential distribution may be at least as good a fit to the central light. Sometimes the bulge region has a boxy shape, just as some ellipticals do, as shown in Figure 5.6.

Almost every disk galaxy with a measured radial profile, including Magellanic irregulars, shows an exponential profile in the disk. In the region beyond the bulge, the brightness decreases approximately exponentially as:

$$\Sigma = \Sigma_0 e^{(-r/r_s)}$$

where Σ_0 is the intercept value, equal to the extrapolated central surface brightness, and r_s is the *scale length*. This is sometimes written in the form $\Sigma = \Sigma_0 e^{-\alpha r}$, where $\alpha = 1/r_s$. Figure 5.7 shows a radial profile for a spiral galaxy.

A scale length is the distance over which light decreases by $1/e$, or by about a factor of one-third. A galaxy with a larger scale length has a slower decrease in brightness than a galaxy with a smaller scale length. In Figure 5.7, the light decreases from 1000 (in arbitrary units) in the center to $(1000/e) = 368$ at a radius of about $0.2 R_{25}$. (It is customary to measure the scale length in terms of R_{25} , so that you do not need to know the distance to the galaxy.) Typically $r_s/R_{25} \approx 0.2-0.3$, so there are 3–5 scale lengths out to R_{25} . That is, spiral arms can usually be traced out to a distance of ~ 4 scale lengths in a galaxy on typical prints. Recent studies indicate that blue scale lengths may sometimes be shorter than near-

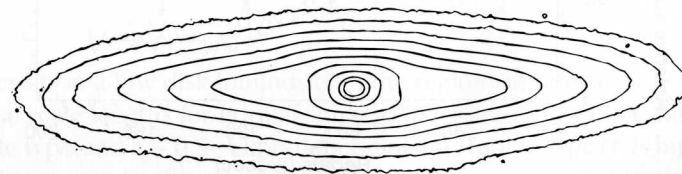


FIGURE 5.6 Magnitude contours are shown for the edge-on spiral galaxy NGC 2310, which has a boxy bulge. (From Shaw 1993.)

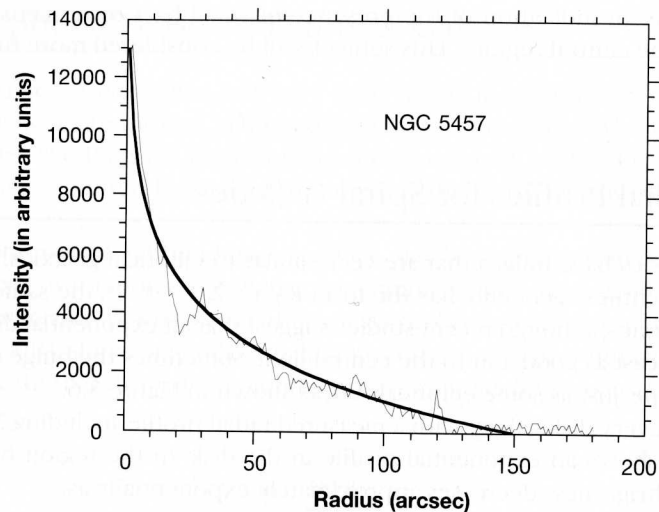


FIGURE 5.7 Radial profile for the spiral galaxy NGC 5457, with a solid curve showing an exponential light profile for comparison.

infrared scale lengths. This fact has consequences for inferred characteristics of the stellar populations as well as dust distributions.

A logarithmic plot of surface brightness versus radius is a straight line whose slope is a measure of the inverse scale length, as shown in Figure 5.8.

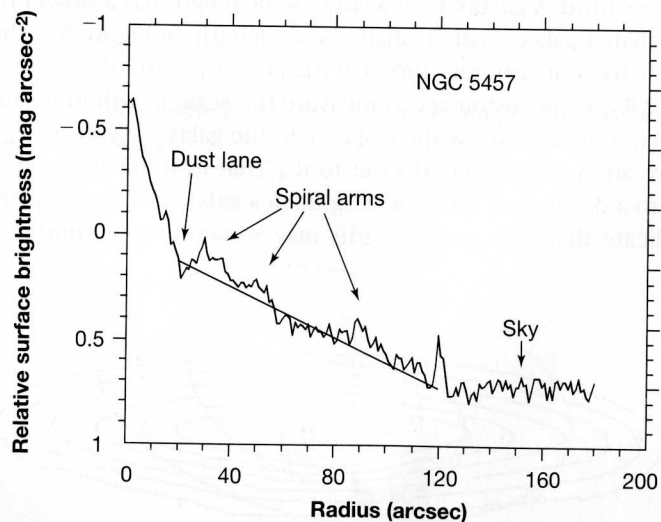


FIGURE 5.8 Logarithmic plot of the radial profile of NGC 5457, compared with the straight line from theory.

In terms of surface brightness, the scale length is given by

$$\mu(r) = \mu_0 + 1.086 \frac{r}{r_s}$$

for central surface brightness μ_0 . This expression results from the use of log (base 10) in defining magnitudes, and ln (base e) in defining scale length: the scale length r_s is given by $r/r_s = \ln \Sigma/\Sigma_0 = 2.3 \log \Sigma/\Sigma_0$. In Figure 5.8, the inverse slope is $1.0/[2.3(3-1)]$, so the scale length is ~ 0.2 , in agreement with the value found from Figure 5.7. The central regions of a galaxy are a combination of an $r^{1/4}$ shape plus an exponential disk. In deep exposures, these regions may be saturated, so the central extrapolated surface intensity may be difficult to determine. With a log plot, the outer slope determines the scale length without needing to know the central surface brightness, so it is easier to use.

The nearby spiral galaxies that are most familiar to us all have the same central blue surface brightness, 21.65 ± 0.3 mag arcsec $^{-2}$; this result is known as *Freeman's law*. Recent results indicate that this is an upper limit rather than an absolute range for spirals, and some have suggested that it is no more than a selection effect. If the central disk surface brightness in normal spirals is approximately constant, the total absolute magnitude of galactic disks is determined by the scale length. Low surface brightness (LSB) galaxies, on the other hand, have typical blue central surface brightnesses of 23.8 mag arcsec $^{-2}$.

Ken Freeman noted that the transition region between the bulge and disk may have either of two forms: Type I has an excess of light just outside the bulge relative to the extrapolated exponential disk; this excess may be due to the presence of a bar or ring. Type II has an apparent dip in the inner disk (also seen in CO in some galaxies; see Chapter 6), which could result from orbit perturbations near a bar or from mass infall to the nucleus. Good empirical fits to Type II profiles can be achieved by combining an $r^{1/4}$ profile with an exponential disk of the form

$$\Sigma = \Sigma_0 \exp \left[-\alpha r + \left(\frac{\beta}{r} \right)^3 \right]$$

which results in a low disk luminosity in the regions interior to β .

Typical scale lengths for normal spiral galaxies are $r_s = 2-5$ kpc, independent of Hubble type, and $r_c \sim 0.5-4$ kpc, depending on Hubble type (r_c is bigger in earlier Hubble types); in all cases, $r_c < r_s$. This relation is observed for LSB galaxies as well. For the Milky Way, the current best estimates for the scale lengths are 5.0 ± 0.5 kpc for r_s and 2.7 kpc for r_c .

TABLE 5.1 *Disk/bulge ratios*

Hubble type	$L_{\text{bulge}}/L_{\text{total}}$	D/B	Hubble type	$L_{\text{bulge}}/L_{\text{total}}$	D/B
Sb	0.45	2.2	Sc	0.15	6.7
Sbc	0.32	3.1	Sd	0.01	100

Source: From Kent 1987 and Boroson 1981.

Typically, more than 75% of the total blue light of a spiral galaxy comes from the disk. An evaluation of the ratio of disk to bulge luminosity (D/B) through an integration of the radial light distributions yields

$$\frac{D}{B} = 0.28 \left(\frac{r_s}{r_c} \right)^2 \frac{\sum_o}{\sum_c}$$

(See Mihalas and Binney 1981 for further details.)

The typical D/B ratio is about 1 for S0 galaxies, but with wide variation; the ratio for Sb galaxies (e.g., M31) is about 3, and for Sc galaxies (e.g., M33) about 12. Table 5.1 gives representative values for disk/bulge ratios, along with bulge-to-total luminosity ratios, based on a decomposition of the radial profiles into the bulge and disk components. For comparison, the Milky Way has a bulge luminosity/total luminosity ratio of 0.34 ± 0.08 , which implies type Sbc. LSB galaxies generally have $D/B > 10$, although a $D/B \sim 1$ is not uncommon.

The perpendicular light profiles of disk galaxies have been measured in edge-on systems. They show an approximately exponential light decrease with increasing z distance that is independent of radial distance from the galactic center in the disk. The disks of some galaxies, particularly S0s, have an extensive flat component referred to as a *thick disk*.

5.5 Radial Profiles for Barred Spiral Galaxies

Barred galaxies, like nonbarred spirals, have exponential disks. There are two types of bars: *Flat bars* have almost constant surface brightness along the bar; that is, they have a much shallower decline than the disk. An example is NGC 1300 shown in Figure 5.9. *Exponential bars*, in contrast, have the same scale length as the disk; an example is NGC 2500 in Figure 4.9.

Figure 5.10 shows the general shape for bar radial profiles. The solid curve indicates the azimuthally-averaged exponential profile for the disk. The profile along the bar is shown by the top line; the bar ends at a radius of about $0.2 R_{25}$ in this figure. Beyond the bar, the line represents the intensity along the spiral arms, which is higher than that along the interarm regions. The light distribution along the exponential bar and the continuation into the spiral arms are shown in the intermediate curve; the bar does not stand out in this case. For compari-



FIGURE 5.9 *Flat-barred galaxy NGC 1300. (Imaged in the B band with the KPNO Burrell-Schmidt telescope. From Elmegreen et al. 1995.)*

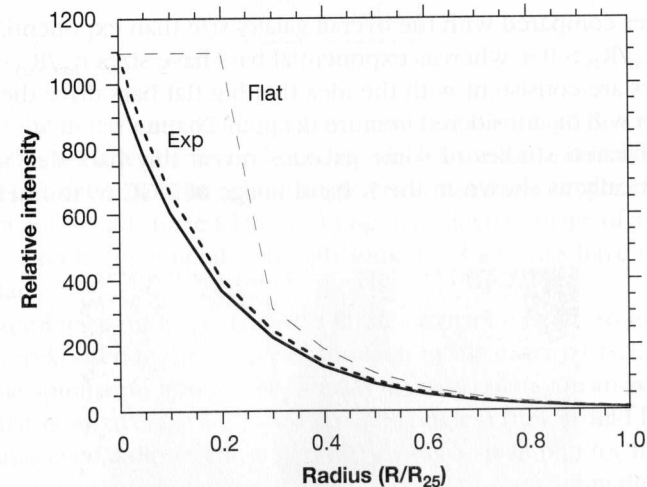


FIGURE 5.10 *Radial profiles in spiral galaxies with strong (flat) and weak (exponential) bars.*

son, radial profiles are shown for the flat-barred galaxy NGC 1300 and the exponential-barred galaxy NGC 1359 in Figure 5.11.

A number of galaxy parameters are correlated with bar type. There is a strong Hubble-type dependence, in the sense that early types usually have flat bars. A strong Arm Class dependence (see Section 5.8) is also present: flat-barred galaxies usually have a grand design spiral structure, whereas exponential-barred galaxies usually are flocculent in their outer disks. Furthermore, flat bars gener-

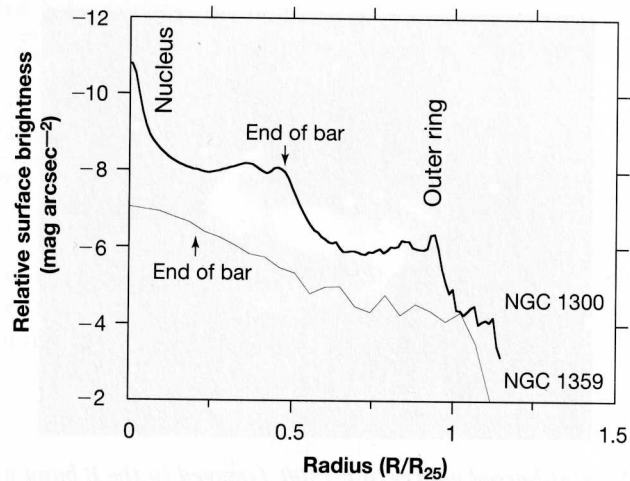


FIGURE 5.11 Radial profiles for the flat-barred galaxy NGC 1300 and the exponential-barred galaxy NGC 1359.

ally are larger compared with the overall galaxy size than exponential bars: Flat bars have $r_{\text{bar}}/R_{25} > 0.4$, whereas exponential bars have sizes $r_{\text{bar}}/R_{25} < 0.3$. All of these factors are consistent with the idea that big flat bars drive the spiral patterns, which will be considered in more detail in Chapter 9.

Recent infrared studies of some galaxies reveal tiny bars that are not detectable optically, as shown in the K band image of NGC 6946 in Figure 5.12.

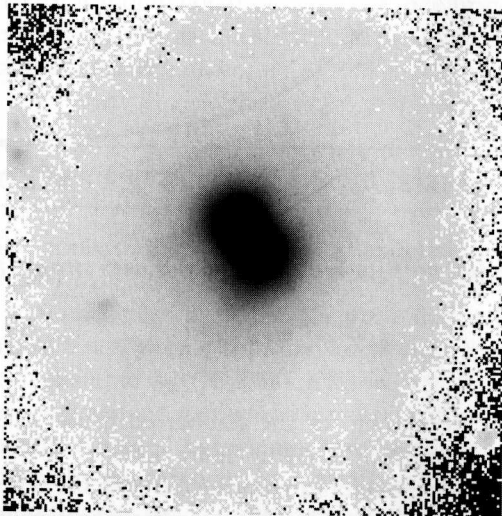


FIGURE 5.12 This K band image of the center of the spiral galaxy NGC 6946 reveals a tiny stellar bar inside the circular region. (From the KPNO 2.1-m telescope, D. Elmegreen and F. Chromey, Vassar College.)

These observations suggest that tiny bars contain very old stars, sometimes obscured by dust at optical wavelengths. Maps of CO distributions often reveal tiny bars in the gas also.

5.6 Image Enhancement

Galaxies are randomly inclined to our line of sight, and high inclinations make it difficult to discern spiral structure. We can simulate face-on aspects by “stretching” images until the galaxies appear round (since disks presumably are circular). Computers facilitate the rectification of images. If the image is stored as an array of numbers (which are picture elements, or *pixels*), deprojection is accomplished by multiplying the pixels along the minor axis by a factor equal to the inverse of the cosine of the inclination, i . The corrected distance along the minor axis, d_c , is then given in terms of its observed distance d_{obs} by

$$d_c = \frac{d_{\text{obs}}}{\cos(i)}$$

Stretching the minor axis on computer is easiest if the image is oriented so that its minor axis is either horizontal or vertical. This orientation is achieved by rotating the galaxy image through an angle equal to its position angle. The major axis, of course, is undistorted. The resulting deprojected image of a spiral galaxy should be circular, in general, although sometimes galaxies have rings that are not circular.

Photographic reproductions have a limited dynamic range, so images usually end up overexposed in the center or too faint in the outer parts. It is important to note that spiral arms appear very weakly on radial plots: On an averaged radial profile (that is, an average over all azimuthal angles) they would hardly be noticeable, and even a direct cut would show only a small blip for most galaxies. The point is that spirals are bright only relative to their immediate neighborhood, typically by about a magnitude or so. The images can be enhanced by removing the azimuthally averaged radial profile from each galaxy and normalizing each radial position to a constant average deviation so that features in both the inner and the outer regions can be seen equally well. This enhancement is done on a digital galaxy image by dividing the intensity of the light at each pixel by the average light at that radius from the galaxy center. The resulting light is normalized at each radius to a constant rms value.

After enhancements, remarkable structure becomes apparent that was hidden in the original images. In the deprojected, radial profile-subtracted image of M81, shown in Figure 5.13, note the narrowing of the two main arms halfway out, where the arm brightness decreases. (Compare this image with the conventional sky view of M81 in Figure 5.16.) This pattern has been noticed in